数理解析研究所講究録
第661巻 1988年 141-158

水波のパラメトリック励振：Nonlinear dynamics and chaos

東大理　神部　勉　(Tsutomu Kambe)
梅木　誠　(Makoto Umeki)
唐津　正之 (Masayuki Karatsu)

1. Introduction

Surface waves of a liquid in a closed basin subjected to horizontal or vertical oscillation have been studied recently from a viewpoint of low-dimensional chaos. Faraday (1831) first studied experimentally the patterns of standing waves in a container which is oscillated vertically and found that the frequency of surface oscillation is one-half of that of the excitation. Based on linear theory, Benjamin & Ursell (1954) explained the excitation of standing waves of an inviscid liquid which is associated with the instability of solutions of Mathieu equation for parametric resonant modes. Ockendon & Ockendon (1973) analysed three types of horizontally or vertically oscillated gravity waves of a finite amplitude and pointed out that the horizontally excited case is closely related to Duffing equation which is now well-known to possessing chaotic solutions, and that in the vertically excited case (briefly called as Faraday problem), there exists a bifurcation from a stable quiescent state to a stable standing wave of a finite amplitude.

Miles (1976) formulated the weakly nonlinear problem of gravity waves. He reduced the kinematical boundary-value problem to a variational problem and introduced Lagrangian and Hamiltonian functions in terms of generalized coordinates of the free surface displacements { η_n }. This formulation is applied to the weakly or resonantly coupled free oscillations, where averaged Lagrangian function is introduced. Analyses of the external-internal parametric resonant surface waves are given in the following works: Faraday problem in Miles (1984a), the internally resonant problem in Miles (1984b), and the horizontally excited problem in Miles (1984c). In the last paper he found chaotic solutions for two degenerated modes which are similar to the system of a pendulum oscillated horizontally. However for Faraday problem with $\omega_1 = 2\omega_2$, no chaotic solution is found.

On the other hand, several experiments have been made and periodic, quasi-periodic, and chaotic wave motions are reported. Keolian et al. (1981) used a narrow Plexiglas annulus and found long-period subharmonic sequences arising from period-doubling. Keolian & Rudnick (1984) used both liquid helium and water and observed quasi-periodic motions and phase locking. Gollub & Meyer (1983) found that an axisymmetric mode breaks down and changes into a non-axisymmetric one as the driving amplitude increases with a fixed frequency. Ciliberto & Gollub (1985) (hereinafter denoted by C&G) examined the case that the driving amplitude and frequency are chosen to be near the intersection of the stability boundaries of two nearly degenerated modes. They found periodic and chaotic competition of two modes characterized as (m,n)=(4,3)

and (7,2) by optical measurement, where mode (m,n) expresses the eigenfunction $J_m(\kappa_{mn}r)\cos m\theta$, $\kappa_{mn}=j'_{mn}/R$, j'_{mn} n-th zero of $J_m(x)$, and R the radius of the circular container. They showed that mode competition occurs in only one side of the phase diagram. They also measured a positive Lyapunov characteristic exponent (LCE) and some fractal dimensions from experimental data.

More recently, Funakoshi & Inoue (1987,1988) studied chaotic motions of surface waves in a circular cylinder subjected to horizontal oscillation and showed that the experimental measurement agrees well with numerical calculation of the dynamical systems derived by Miles (1984c). We made an experiment on Faraday problem and found that there exists a competition of two modes (4,1) and (1,2) different from C&G's case.

We studied the Faraday problem of subharmonic mode competition of (m_1,n_1) and (m_2,n_2) where $m_i \pm m_j \pm m_k \neq 0$, for i,j,k=1,2, including C&G's and our experiments. We derive the dynamical systems for two modes, analysed them numerically and found that periodic mode competing solutions, period-doubling bifurcation and chaotic solutions exist on the same side in the phase diagram as C&G found chaotic motions. All LCEs are computed and it is shown that there exists one positive maximal LCE in the chaotic region. Meron & Procaccia (1986,1987) analysed C&G's experiment by normal form and center manifold theory but their systems are equivalent to our result derived by Miles' formulation.

2. Dynamical systems of surface waves

We consider weakly nonlinear surface waves of an inviscid liquid in a closed basin. Let (x,y) and z be horizontal and vertical coordinates in a reference frame fixed in a basin B with a cross section S and n being the outward normal, $z=\eta(x,y)$ the free surface, z=-d the bottom and d the depth of the undisturbed fluid. We assume that the motion is irrotational so that the velocity relative to B is expressed by a velocity potential $\phi(x,y,z)$ as $v=\nabla\cdot\phi$.

We may obtain the solution in the form

$$\phi = \sum_n \phi_n(t)\,\psi_n(x,y)\,H_n(z), \tag{2.1a}$$

$$\eta = \sum_n \eta_n(t)\,\psi_n(x,y), \tag{2.1b}$$

where ψ_n are the eigenfunctions of the linear system;

$$\left(\frac{\partial^2}{\partial x^2}+\frac{\partial^2}{\partial y^2}+K_n^2\right)\psi_n = 0, \tag{2.2a}$$

with $n\cdot\nabla\psi_n = 0 \quad on \quad \partial S,$ (2.2b)

$$\int_S \psi_m\psi_n\,dx\,dy = S\cdot\delta_{mn} \tag{2.2c}$$

where δ_{mn} is the Kronecker delta, ∂S is the boundary of S and $H_n(z) = \operatorname{sech} K_n d \cosh K_n z$

Miles(1976) reduced the kinematical boundary-value problem to the variational problem of the integral

$$I = \frac{1}{2}\int_V (\nabla\phi)^2\,dx\,dy\,dz - \int_S \phi(z=\eta)\cdot\eta_t\,dx\,dy \tag{2.3}$$

with respect to $\delta\phi$ for given η_t . This is equivalent to Dirichlet's principle that the velocity field v satisfying div v =0 gives the minimal value of I among all irrotational flows occupying a bounded simply connected region V.

Substituting (2.1a,b) into the integral I, we obtain

$$S^{-1}I = \frac{1}{2}k_{mn}\phi_m\phi_n - d_{mn}\dot{\eta}_m\phi_n \tag{2.4}$$

where

$$k_{mn} = S^{-1}\int_V \nabla\psi_m\cdot\nabla\psi_n H_m(z) H_n(z)\,dx\,dy\,dz \qquad (2.5a)$$

and

$$d_{mn} = S^{-1}\int_s \psi_m \psi_n H_n(z=\eta)\,dx\,dy. \qquad (2.5b)$$

The variational principle yields

$$\frac{\partial}{\partial\phi_n} I = 0 \qquad (2.6)$$

which relates $\{\phi_n\}$ and $\{\eta_n\}$ as

$$\phi_n = l_{nm}(\eta)\dot{\eta}_m, \qquad (2.7)$$

where $l_{nm}=d_{nl}k_{lm}^{-1}$ and dots mean the differential with respect to time.

Averaged Lagrangian is constructed in terms of $\{\eta_n\}$ including a capillary effect. The kinematic energy of the fluid is given by

$$T = \frac{1}{2}\rho\int_V (\nabla\phi)^2\,dx\,dy\,dz$$

$$= \frac{1}{2}\rho S k_{mn}\phi_m\phi_n = \frac{1}{2}\rho S a_{mn}\dot{\eta}_m\dot{\eta}_n, \qquad (2.8)$$

where $a_{mn} = l_{im}k_{ij}l_{jn}$. (2.9)

Expanding a_{mn} leads to

$$a_{mn} = \delta_{mn}a_m + a_{lmn}\eta_l + \frac{1}{2}a_{jlmn}\eta_j\eta_l + \cdots, \qquad (2.10)$$

where $a_n = k_n^{-1} = (K_n \tanh K_n d)^{-1}$ (2.11)

$$a_{lmn} = C_{lmn} - D_{lmn}a_m a_n \qquad (2.12)$$

$$a_{jlmn} = -D_{jlmn}(a_m+a_n) + 2D_{jmi}D_{lni}a_i a_m a_n \qquad (2.13)$$

$$C_{lmn} = S^{-1}\int_s \psi_\ell\psi_m\psi_n\,dx\,dy, \quad C_{jlmn} = S^{-1}\int_s \psi_j\psi_\ell\psi_m\psi_n\,dx\,dy, \qquad (2.14a,b)$$

and $D_{lmn} = S^{-1}\int_s \psi_\ell\nabla\psi_m\cdot\nabla\psi_n\,dx\,dy$, $D_{jlmn} = S^{-1}\int_s \psi_j\psi_\ell\nabla\psi_m\cdot\nabla\psi_n\,dx\,dy$. (2.15a,b)

The potential energy due to the free surface displacement is

$$V = \rho\int_s dx\,dy\int_0^\eta g\cdot z\,dz$$

$$= -\rho S\left(Q_n\eta_n + \frac{1}{2}g_z\eta_n^2\right), \qquad (2.16)$$

where $Q_n = -\int_s (g_x x + g_y y)\,dx\,dy$, (2.17)

and $g_z = -g + g_0\cos 2\omega t$. (2.18)

The capillary energy due to the surface tension γ is

$$V_c = \frac{1}{2}\gamma \int_S [\{1+(\nabla\eta)^2\}^{\frac{1}{2}} - 1]\, dx\,dy$$
$$= \frac{1}{2}\gamma S K_n^2 \eta_n^2 - \frac{1}{8}\gamma S E_{jlmn}\eta_j\eta_l\eta_m\eta_n + \cdots, \qquad (2.19)$$

where

$$E_{jlmn} = S^{-1}\int_S (\nabla\psi_j\cdot\nabla\psi_l)\cdot(\nabla\psi_m\cdot\nabla\psi_n)\, dx\,dy, \qquad (2.20)$$

which arises from nonlinearity of the capillary effect. We assume that this term is less dominant than other nonlinear terms in (2.8). Lagrangian function devided by ρ S is given by

$$L = \frac{1}{\rho S}(T - V - V_c)$$
$$= \frac{1}{2}a_{mn}\dot{\eta}_m\dot{\eta}_n - \frac{1}{2}\{(1+\lambda^2K_n^2)g - g_0\cos 2\omega t\}\eta_n^2 + Q_n\eta_n \qquad (2.21)$$

where is a capillary length and about 2.8(mm) for clean water. Q_n vanishes for Faraday problem.

Here we assume the amplitude of the displacement of the n-th mode is of the form

$$\eta_n = p_n(\tau)\cos\omega t + q_n(\tau)\sin\omega t + A_n(\tau)\cos 2\omega t + B_n(\tau)\sin 2\omega t + C_n(\tau) \qquad (2.22)$$

where subharmonic modes $p_n = q_n = 0$ except n=1 and 2, p_n, q_n $= O(\varepsilon)$, A_n, B_n, C_n $= O(\varepsilon^2)$, and $\tau = \varepsilon^2\omega t$ is a slowly varying time. Substituting (2.20) into (2.18) and averaging with respect to t over $2\pi/\omega$ yield

$$\langle L\rangle = \frac{1}{2}a_n\omega^2\Big[(\dot{p}_n q_n - p_n\dot{q}_n) + \frac{1}{2}(1-\omega_n^2/\omega^2)(p_n^2+q_n^2)$$
$$+ \frac{1}{4}\frac{g_0k_n}{\omega^2}(p_n^2-q_n^2) + 2(1-\omega_n^2/4\omega^2)(A_n^2+B_n^2) - \frac{\omega_n^2}{\omega^2}C_n^2$$
$$+ k_n(a_{lmn} - \frac{1}{4}a_{nlm})\{(p_lp_m - q_lq_m)A_n + (p_lq_m + q_lp_m)B_n\}$$
$$+ \frac{1}{2}k_n a_{nlm}(p_lp_m + q_lq_m)C_n$$
$$+ \frac{1}{32}k_n(a_{jlmn} + a_{jlnm})\{(p_jp_l + q_jq_l)(p_mp_n + q_mq_n)$$
$$+ 2(p_lq_m - q_lp_m)(p_jq_n - q_jp_n)\}\Big] \qquad (2.23)$$

where

$$\omega_n = \{ k_n g (1 + \lambda^2 K_n^2) \}^{\frac{1}{2}} \qquad (2.24)$$

is a natural frequency of the n-th mode. Requiring <L> to be stationary with respect to A_n, B_n, and C_n yields

$$(A_n, B_n) = - \frac{1}{4} k_n (1 - \omega_n^2 / 4\omega^2)^{-1} (a_{lmn} - \frac{1}{4} a_{nlm}) \times (p_l p_m - q_l q_m , p_l q_m + q_l p_m), \qquad (2.25a,b)$$

$$C_n = \frac{k_n \omega^2}{4 \omega_n^2} a_{nlm} (p_l p_m + q_l q_m). \qquad (2.26)$$

Using (2.25a,b) and (2.26), averaged Lagrangian is expressed as

$$\langle L \rangle = \frac{1}{2} (\dot{p}_n q_n - p_n \dot{q}_n) + H \qquad (2.27)$$

where p_n, q_n are normalized by a factor $\sqrt{\frac{a_n}{g}}\omega$ for n=1, 2, <L> is devided by g and H is a Hamiltonian function with q_n, p_n being conjugate coodinates and momenta:

$$H = \frac{1}{2} (\Omega_n p_n^2 + \Omega_n' q_n^2) - a_n (1 - \omega_n^2 / 4\omega^2) (A_n^2 + B_n^2) + a_n \omega_n^2 / 2\omega^2 C_n^2 + \frac{1}{64} (a_{jlmn} + a_{jlnm}) \{ (p_j p_l + q_j q_l) (p_m p_n + q_m q_n) + 2 (p_l q_m - q_l p_m) (p_j q_n - q_j p_n) \}, \qquad (2.28)$$

where $\Omega_n = \frac{1}{2\omega^2} (\omega^2 - \omega_n^2 + \frac{g_0}{2} k_n)$, (2.29a)

and $\Omega_n' = \frac{1}{2\omega^2} (\omega^2 - \omega_n^2 - \frac{g_0}{2} k_n)$. (2.29b)

The evolution equations for p_n, q_n are expressed by Hamilton's equation. Calculating H for explicit modes $1=(m_1,n_1)$ and $2=(m_2,n_2)$ with m_i m_j m_k 0 for i, j, k =1 or 2 yields

$$H(p_1,q_1,p_2,q_2) = \frac{1}{2} (\Omega_n p_n^2 + \Omega_n' q_n^2) + \frac{1}{4} b_n (p_n^2 + q_n^2)^2 + \frac{1}{2} c (p_1^2 + q_1^2) (p_2^2 + q_2^2) + \frac{1}{2} e (p_1 q_2 - p_2 q_1)^2, \qquad (2.30)$$

where b_n, c and e are constants which depends on d and R. Simple estimation leads to

$$b_1 \simeq b_2 \simeq c \simeq d/1.6 \qquad (2.31)$$

(see Umeki(1988) for detail).

Although the inviscid theory leads to Hamiltonian systems,

real motion of surface waves is dissipative. So we may add the linear damping terms phenomenologically as $(-\alpha_1 p_1, -\alpha_1 q_1, -\alpha_2 p_2, -\alpha_2 q_2)$. α_n are determined so as to reproduce the stability boundaries in C&G's experiment. Then we study the dissipative nonlinear dynamical systems of the form

$$\dot{p}_1 = -\alpha_1 p_1 + (-\Omega_1' + r_1^2 + r_2^2) q_1 - b M p_2 \quad (2.32a)$$

$$\dot{q}_1 = -\alpha_1 q_1 + (\Omega_1 - r_1^2 - r_2^2) p_1 - b M q_2 \quad (2.32b)$$

$$\dot{p}_2 = -\alpha_2 p_2 + (-\Omega_2' + r_1^2 + r_2^2) q_2 + b M p_1 \quad (2.32c)$$

$$\dot{q}_2 = -\alpha_2 q_2 + (\Omega_2 - r_1^2 - r_2^2) p_2 + b M q_1, \quad (2.32d)$$

where $r_n^2 = p_n^2 + q_n^2$, $M = p_1 q_2 - p_2 q_1$ and $b = 1.6$.

3. Stability analysis

We consider the system with parameters chosen so as to be consistent with C&G's experiment. Fixed points of (2.32a-d) are given by

$$(p_1, q_1, p_2, q_2) = (0, 0, 0, 0) \quad (3.1a)$$

$$= \pm (p_{1-}^*, q_{1-}^*, 0, 0) \quad (3.1b)$$

$$= \pm (p_{1+}^*, q_{1+}^*, 0, 0) \quad (3.1c)$$

$$= \pm (0, 0, p_{2-}^*, \quad) \quad (3.1d)$$

$$= \pm (0, 0, p_{2+}^*, q_{2+}^*) \quad (3.1e)$$

where

$$p_{n\pm}^* = (r_{n\pm}^* - \Omega_n') r_{n\pm}^* / \{(r_{n\pm}^* - \Omega_n')^2 + \alpha_n^2\}^{1/2} \quad (3.2a)$$

$$q_{n\pm}^* = \alpha_n r_{n\pm}^* / \{(r_{n\pm}^* - \Omega_n')^2 + \alpha_n^2\}^{1/2} \quad (3.2b)$$

and

$$r_{n\pm}^* = \left[\frac{1}{2}\left\{\Omega_n + \Omega_n' \pm \left((\Omega_n + \Omega_n')^2 - 4(\Omega_n \Omega_n' + \alpha_n^2)^{\frac{1}{2}}\right\}\right]^{\frac{1}{2}}$$

$$= \left[\frac{1}{2}\left\{1 - \omega^2/\omega_n^2 \pm \left(\left(\frac{g_0 k_n}{2\omega^2}\right)^2 - 4\alpha_n^2\right)^{\frac{1}{2}}\right\}\right]^{\frac{1}{2}} \quad (3.2c)$$

Other fixed points with all non-zero components may be exist.

If we consider the evoluion of the same (m,n) modes

different only in an athimuthal phase of $\pi/2$, because of $\Omega_1 = \Omega_2$ and $\Omega_1' = \Omega_2'$, it is shown that the angular momentum M will be dissipated:

$$M = M_0 e^{-4\alpha\tau}, \tag{3.3}$$

where M_0 is an initial angular momentum and $\alpha_1 = \alpha_2 \equiv \alpha$. (Note that it is not proved the angular momentum of two degenerated azimuthal cosine and sine components vanishes if we consider two modes of (m_1,n_1), (m_2,n_2) each of which has cosine and sine components, but here we assume that this breaking of the degeneracy is less dominant and consider only two modes expressed azimuthally by cosine.)

Linear stability of the fixed points are determined by considering the roots of the equation requiring the determinant of the linear equations of small perturbations $(p_1, q_1, p_2, q_2)\, e^{\lambda\tau}$ to vanish. Stability diagram calculated with parameters we chose is shown in figure 1. We devide the phase diagram into six regions labelled as I, II, ..., VI by numbers of fixed points. In any region the fixed point (3.1a) exists and its stability boundary is shown by a solid line, which is equivalent to the transition curves of damped Mathieu equation.

In the region (I), there are one stable fixed point (3.1e) and one unstable fixed point (3.1d) except (3.1a). Although the state at rest is stable, if the (4,3) mode is excited in other parameter region and then the parameter is changed into this region, the (4,3) mode will continue to be excited.

In the region (II), a stable fixed point (3.1e) exists and (3.1a) is unstable with the instability direction (4.3) mode. So if we begin to oscillate the basin filled with still water, the

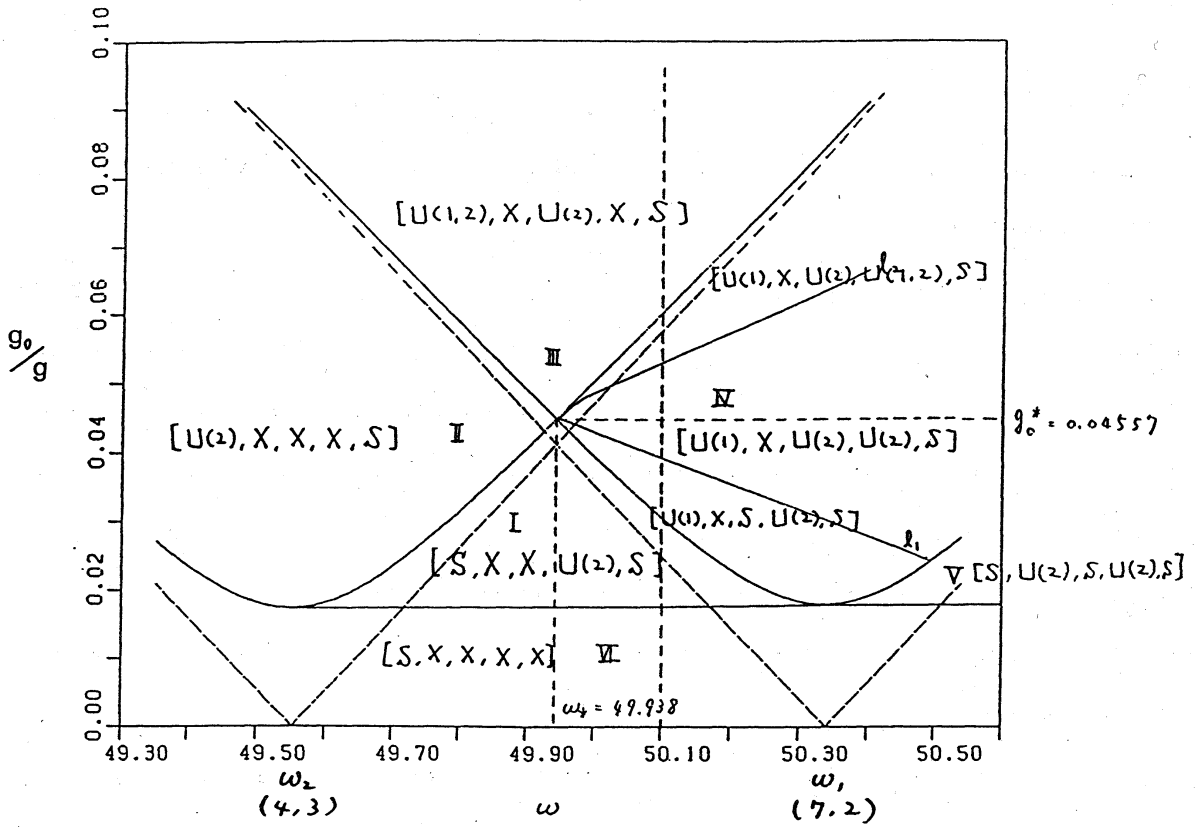

Figure 1. Stability diagram for (7,2) and (4,3) modes. Fixed points (3.1a-e) are in order in the brace. X;not exist, S;exists and stable, U(n);exists and unstable in the direction of n-th mode.

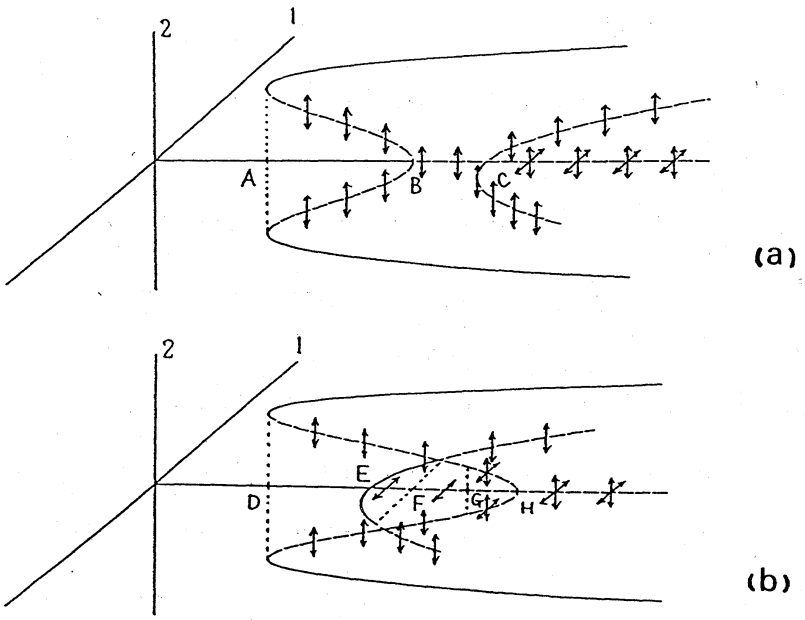

Figure 2. Schematic bifurcation diagrams for (a) $\omega_2 < \omega < \omega_*$ and (b) $\omega_* < \omega < \omega_1$.

(4,3) mode will be excited.

There exist one unstable fixed point (3,1c) and one stable fixed point (3.1e) in the region (III). The (4,3) mode will be excited as well as the region (II).

In the region (IV), there exist three fixed points except (3.1a). One is an unstable (4,3) mode (3.1d), another is a stable (4,3) mode (3.1e), and the other is the (7,2) mode (3.1c). And the stability of the (7,2) mode changes when the parameters cross the line l_1. The (7,2) mode is stable under l_1 and unstable over it. This suggests that there exist bifurcations and chaotic motions just over the line l_1. If the parameter crosses the line l_2, the direction of the instability of (3.1d) changes from (4,3) into (4,3) and (7,2).

All fixed points exist in the region (V). Stable fixed points are (3.1a), (3.1c), (3.1e) and unstable fixed points are (3.1b) and (3.1d). In the region (VI), the only fixed point is (3.1a) and it is stable. No standing wave will not be excited. Note that the change of the stability of nontrivial fixed points occurs only in the region (V), in which C&G found chaotic motions.

Figures 2a,b show schematic bifurcation diagrams obtained by stability analysis of fixed points (3.1a-e) for $\omega_2 < \omega < \omega_*$ and $\omega_* < \omega < \omega_1$, where ω_* is the value of ω at the point of the intersection of two stability lines. Solid and dashed lines show stable and unstable fixed points respectively. The arrows indicate the direction of instability. In fig. 2a, B is a subcritical bifurcation point and C is a supercritical pitchfork

one. There is no Hopf bifurcation in this region. But in fig.4b, E is a pitchfork one, H is a subcritical one and F is another new bifurcation point. It suggests the possibility that there exists a periodic solution near F arising from a Hopf bifurcation.

4. Numerical results

We calculate the dynamical systems (2.32a-d) by using a Runge-Kutta and Runge-Kutta-Gill routine of the fourth order. It is confirmed that solutions don't change qualitatively even if t is changed.

Figure 3 shows a bifurcation diagram obtained numerically by plotting the value of M at the points $\dot{p}_i = 0$ with ω = 50.1 (rad/sec). The initial condition is taken as (10^{-4}, 0, 10^{-4}, 0). When g_0/g reaches 0.03897, the fixed point (3.1c) turns unstable (see fig.1) and a new fixed point with all nonzero components appears. At g_0/g =0.0403, it also changes unstable, a Hopf bifurcation occurs, and the periodic mode competition between (7,2) and (4,3) modes begins. At g_0/g =0.04147, a period-doubling bifurcation (gluing bifurcation) occurs and at g_0/g = 0.04261, the motion changes chaotic. In the chaotic region g_0/g = 0.04261 and 0.0441, there exist periodic windows. In several periodic windows inverse period - doubling bifurcations occur. The stable (4,3) mode occurs at g_0/g = 0.0441.

Projection of typical attractors of solutions with ω = 50.1 are shown in figures 4a-d. The systems (2.32a-d) are invariant under the symmetry transforms $(P_1, P_2) \rightarrow (P_1, -P_2)$, $(-P_1, P_2)$ and $(-P_1, -P_2)$ where $P_n = (p_n, q_n)$. Thus, if the systems have solutions $(P_1, P_2)\ (t, P_1^0, P_2^0)$ where P_1^0, P_2^0 are the initial

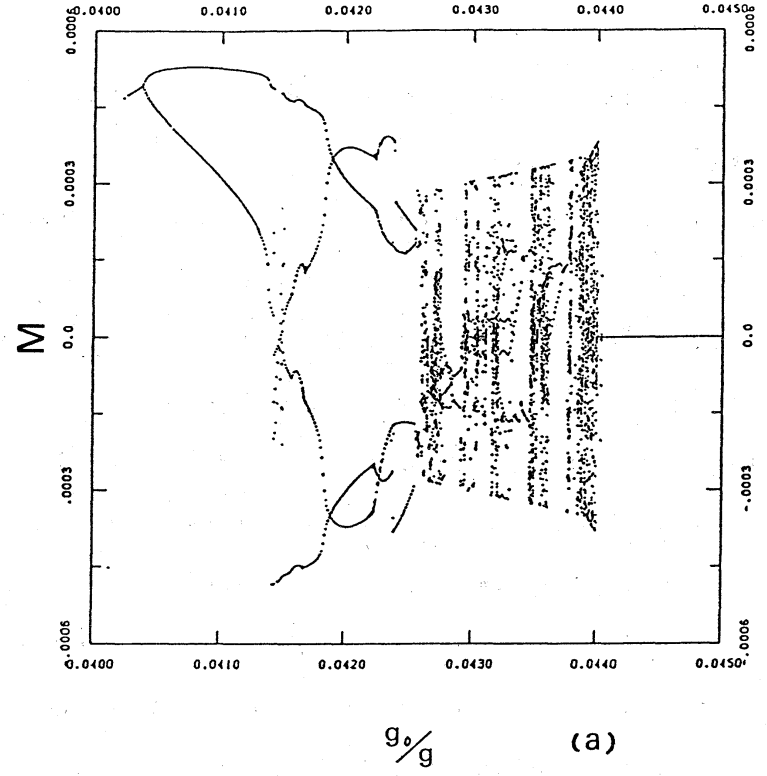

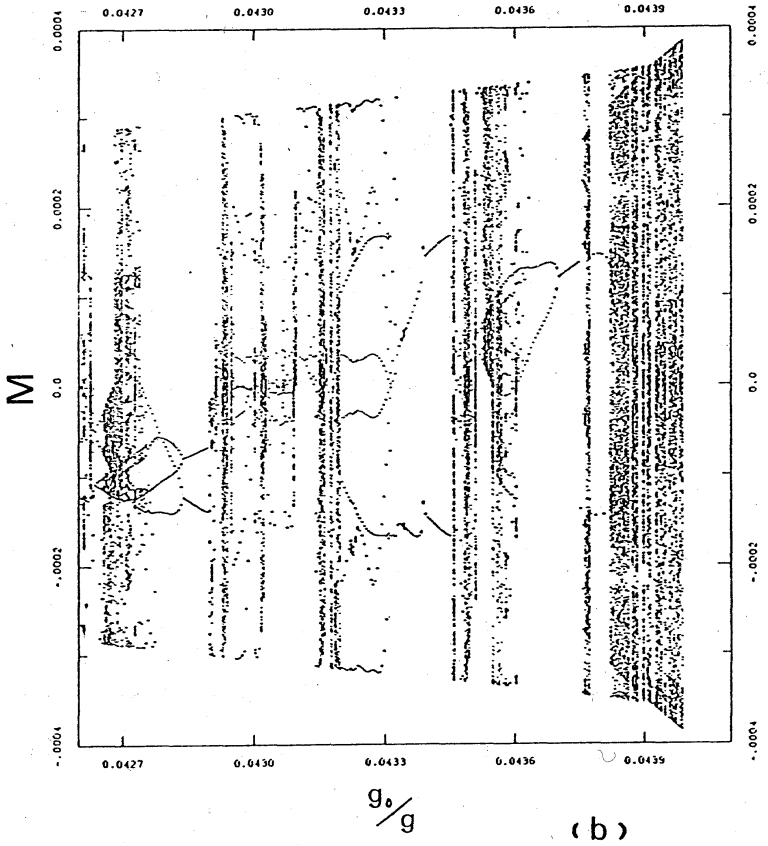

Figure 3. Bifurcation diagram obtained by plotting M at $p_1=0$ of attracters. (a) $0.0403<g_0/g<0.0441$ and (b) the chaotic region enlarged.

condition, they also have solutions $(P_1, P_2)\ (t,P_1^0,-P_2^0)$, $(P_1, P_2)\ (t,-P_1^0,P_2^0)$, and $(P_1, P_2)\ (t,-P_1^0,-P_2^0)$. In fig. 4 a periodic attractor is projected in (p_1, p_2) planes respectively. A period-doubling bifurcation occurred by merging two periodic attractor $(P_1, P_2)\ (t,P_1^0,P_2^0)$ and $(P_1, P_2)\ (t,P_1^0,-P_2^0)$ into one periodic one with double period is shown in figure 4b.

Figure 4c shows an attractor of a periodic solution in a periodic window of the chaotic region with a period four times longer than in fig. 4a. The symmetry with respect to (p_2, q_2) plane is broken. A chaotic attractor is shown in figure 4d. All four attractors are merged into one in this parameter region. The power spectra of p_2 are calculated in figures 5a-d. We see increase of components of low frequencies as g_0 is changed, and an almost continuous spectrum when g_0 is in the chaotic region.

To measure the orbital instability of chaotic solutions, we calculated all LCEs by integrating the linear nonautonomous ODEs of the first variation with reorthonormalization after each time step to avoid numerical divergence. LECs are ordered as $\lambda_1 > \lambda_2 > \lambda_3 > \lambda_4$. Note that the sum of all LCEs is the divergence of the flow (2.32).

Figure 6 shows temporal convergence of all LCEs with ω = 50.1 and g_0/g = 0.0438 (periodic solution), 0.0440 (chaotic solution) and 0.0441 (fixed point). For a periodic solution, the maximal LCE λ_1 is zero and the others are all negative. For a chaotic solution, λ_1 is positive with $\lambda_1/|\lambda_4| \ll 1$, the second λ_2 is zero, and the others are negative. For a fixed point, all LCEs are negative. The variations of LCEs when g_0 is

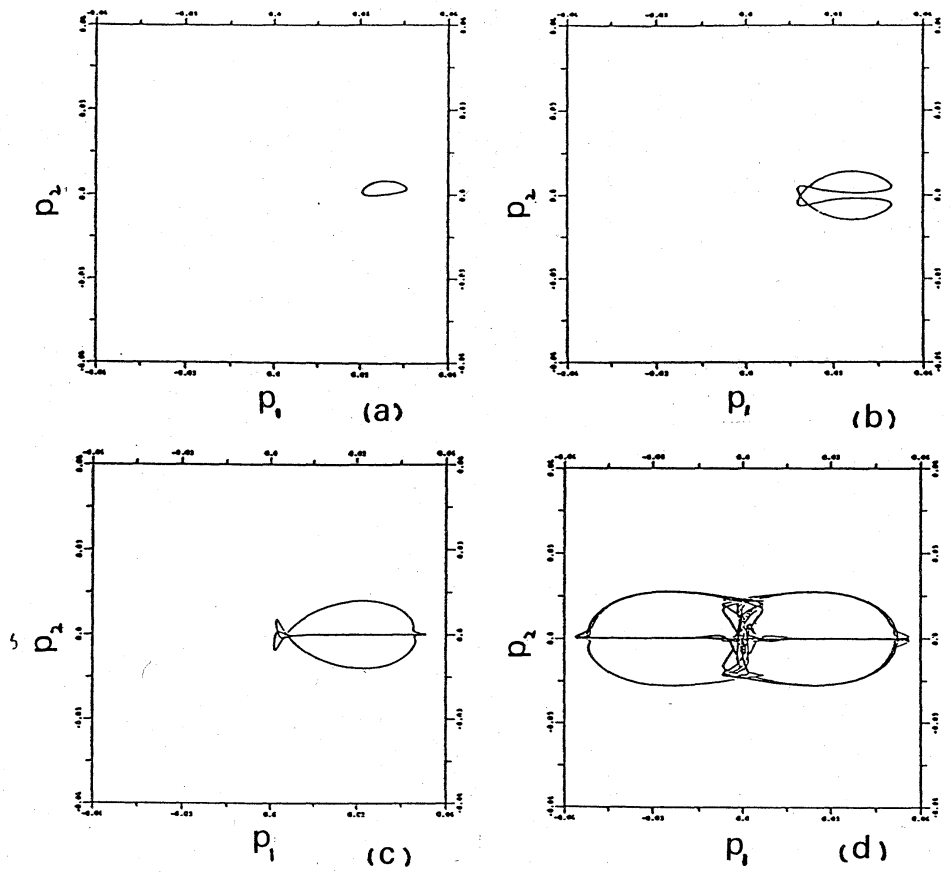

Figure 4. Projections of attractors on (p_1,p_2) plane. ω =50.1 and g_0/g= (a)0.0410, (b)0.0420, (c)0.0430 and (d) 0.0440.

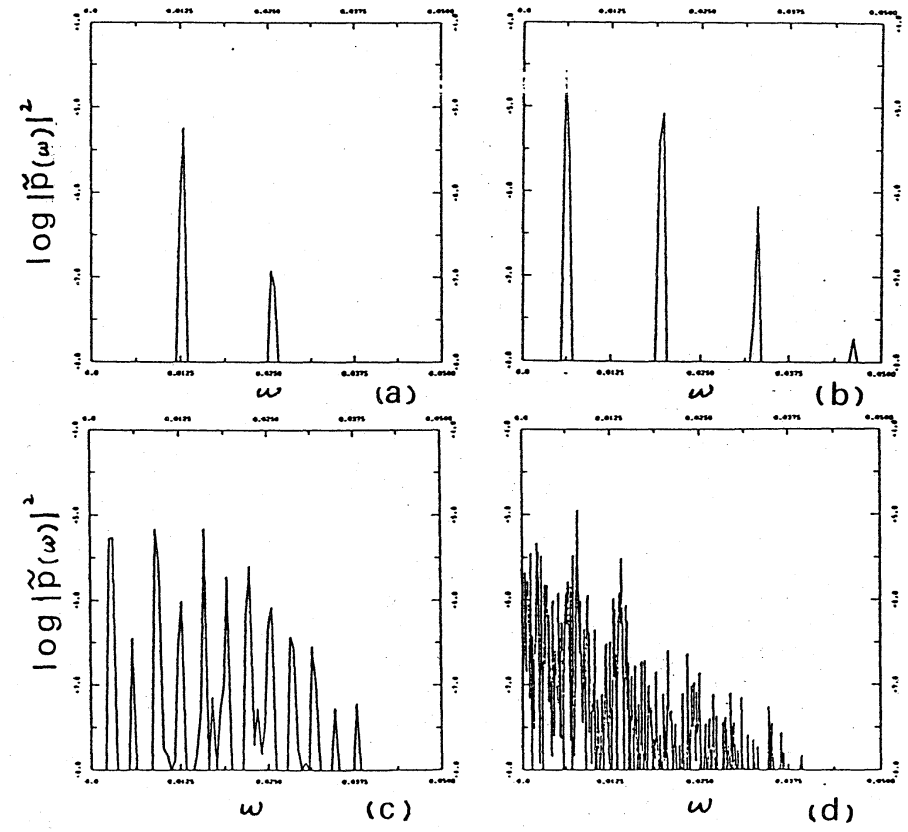

Figure 5. Power spectra of p_2 in fig.4a-d.

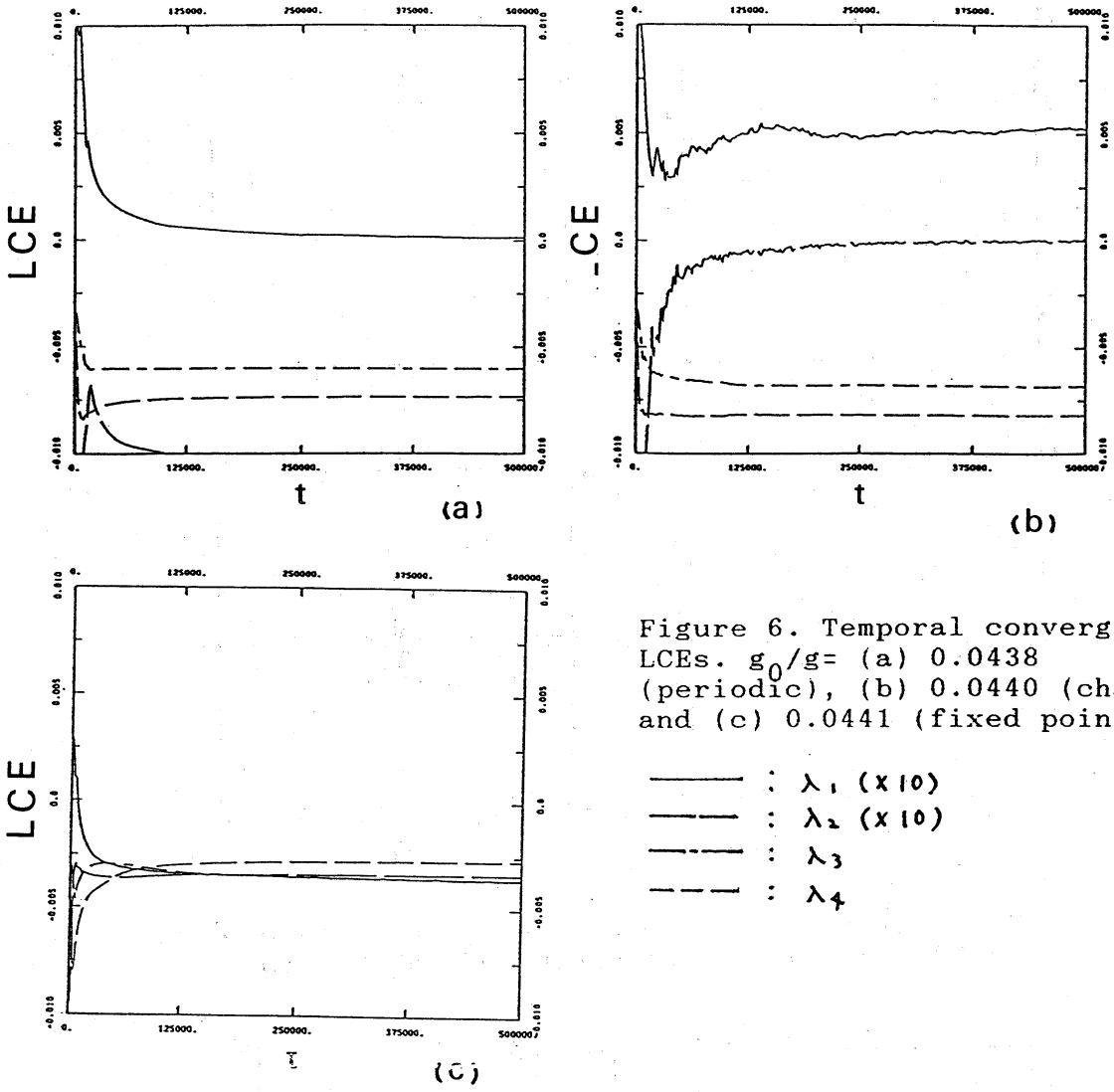

Figure 6. Temporal convergence of LCEs. g_0/g= (a) 0.0438 (periodic), (b) 0.0440 (chaotic) and (c) 0.0441 (fixed point).

——— : λ_1 (x10)
——— : λ_2 (x10)
——·——· : λ_3
— — — : λ_4

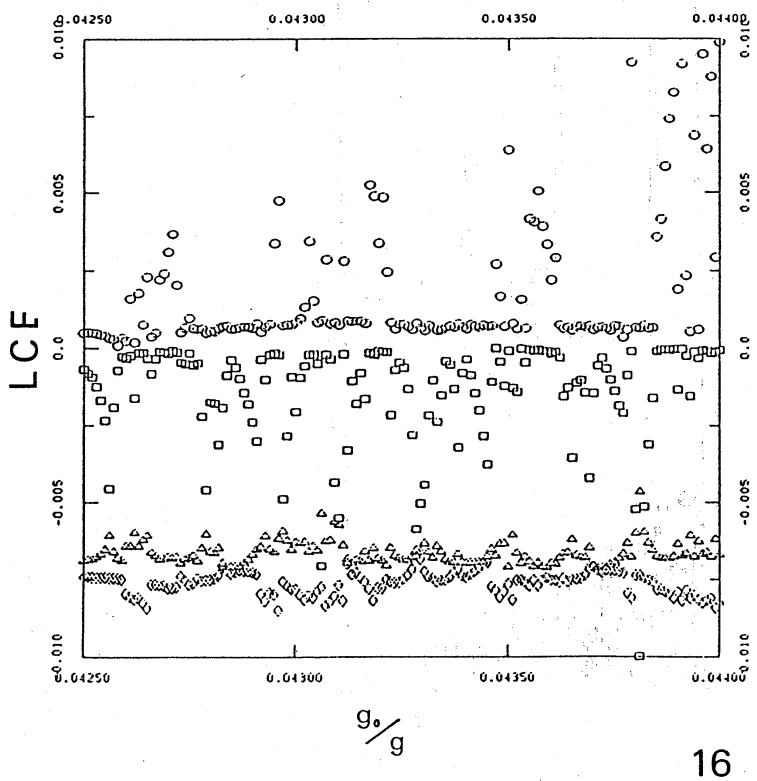

Figure 7. Variation of LCEs in the chaotic region.

o : λ_1 (x 20)
□ : λ_2 (x 5)
△ : λ_3
◇ : λ_4

in the chaotic region are shown in figure 7. Periodic windows in the chaotic region correspond well to those in the bifurcation diagram.

Lyapunov dimension defined by Kaplan and Yorke is expressed by

$$d_L = k + \sum_{i=1}^{k} \lambda_i / |\lambda_{k+1}| \qquad (4.1)$$

where k is the largest value for which $\sum_{i=1}^{k} \lambda_i \geq 0$. From fig. 9 $d_L \simeq 2.1$ in the chaotic region.

References

Benjamin,T.B. & Ursell,F. 1954 The stability of the plane free surface of a liquid in vertical periodic motion. Proc.R.Soc.Lond. A225,505-517.

Ciliberto,S. & Gollub,J.P. 1984 Pattern competition leads to chaos. Phys.Rev.Lett. 52,922-925.

Ciliberto,S & Gollub,J.P. 1985 Chaotic mode competition in parametrically forced surface waves. J. Fluid Mech. 158,381-398.

Faraday,M.1831 On the forms and states assumed by fluids in contact with vibrating elastic surfaces. Phil.Trans. R.Soc.Lond. 121,39-346.

Funakoshi,M. & Inoue,S. 1987 Chaotic behaviour of resonantly forced surface waves. Physics letters A. 121,229-232.

Funakoshi,M. & Inoue,S. 1988 Surface waves due to resonant horizontal oscillation (to appear in J. Fluid Mech.)

Gollub, J.P. & Meyer, C.W. 1983 Symmetry breaking instabilities on a fluid surface. Physica 6D,337-346.

Keolian,R. & Rudnick,I. 1984 The role of phase locking in

quasiperiodic surface waves on liquid helium and water. Proceedings of the International School of Physics. Frontiers in Physical Acoustics. edited by D. Sette. North-Holland, 189-199.

Keolian,R., Turkevich,L.A., Putterman,S.J., & Rudnick,I. 1981 Subharmonic sequences in the Faraday experiment: departures from period-doubling. Phys. Rev. Lett. 47,1133-1136.

Meron,E. & Procaccia,I. 1986 Low-dimensional chaos in surface waves: Theoretical analysis of an experiment. Phys. Rev. A. 34, 3221-3237.

Meron,E & Procaccia,I. 1987 Gluing bifurcations in critical flows: The route to chaos in parametrically excited surface waves. Phys. Rev. A. 35,4008-4011.

Miles,J.W. 1976 Nonlinear surface waves in closed basins. J.Fluid Mech. 75,419-448.

Miles,J.W. 1984a Nonlinear Faraday resonance. J.Fluid Mech. 146,285-302.

Miles,J.W. 1984b Internally resonant surface waves in a circular cylinder. J.Fluid Mech. 149,1-14.

Miles,J.W. 1984c Resonantly forced surface waves in a circular cylinder. J.Fluid Mech. 149,15-31.

Umeki,M. 1988 Nonlinear dynamics and chaos in parametrically excited surface waves. Master thesis (Univ. of Tokyo)